Article

Cell Reports

The Receptor Tyrosine Kinase AXL Is Required at Multiple Steps of the Metastatic Cascade during HER2-Positive Breast Cancer Progression

Graphical Abstract

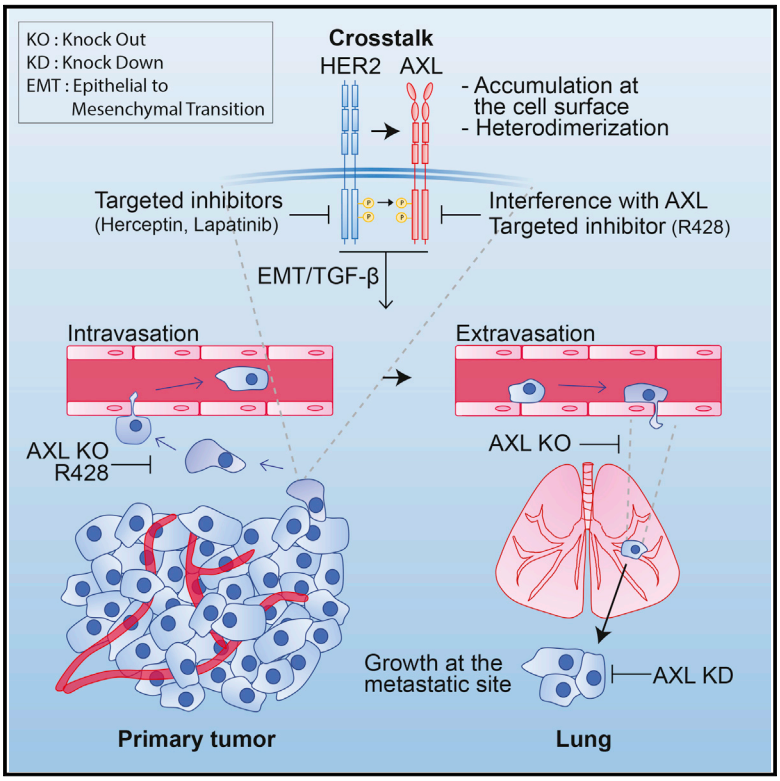

Authors

Marie-Anne Goyette, Stéphanie Duhamel, Léo Aubert, ..., Philippe P. Roux, Jean-Philippe Gratton, Jean-François Côté

Correspondence

jean-francois.cote@ircm.qc.ca

In Brief

Metastasis is responsible for the majority of breast cancer deaths. Goyette et al. report that AXL is expressed in HER2$^+$ human tumors that acquire aggressive features. Blockade of AXL in mice decreases metastasis. These results suggest that co-targeting AXL and HER2 may limit the metastatic progression of HER2$^+$ breast cancer.

Highlights

- AXL expression correlates with poor outcome of HER2$^+$ breast cancer patients
- Co-signaling of HER2 and AXL mediates metastasis of HER2$^+$ breast cancer
- AXL promotes the mesenchymal phenotypes of HER2$^+$ cancer cells for metastasis
- Pharmacological inhibition of AXL reduces metastasis in HER2$^+$ breast cancer mice

Data and Software Availability

GSE102370

Goyette et al., 2018, Cell Reports *23*, 1476–1490
May 1, 2018
https://doi.org/10.1016/j.celrep.2018.04.019

CellPress

OPEN ACCESS
CellPress

Cell Reports
Article

The Receptor Tyrosine Kinase AXL Is Required at Multiple Steps of the Metastatic Cascade during HER2-Positive Breast Cancer Progression

Marie-Anne Goyette,[1,2] Stéphanie Duhamel,[1] Léo Aubert,[3] Ariane Pelletier,[1] Paul Savage,[4] Marie-Pier Thibault,[1] Radia Marie Johnson,[4] Peter Carmeliet,[5,6] Mark Basik,[7] Louis Gaboury,[8] William J. Muller,[4] Morag Park,[4] Philippe P. Roux,[3,8] Jean-Philippe Gratton,[9] and Jean-François Côté[1,2,10,11,12,*]

[1]Montreal Clinical Research Institute (IRCM), Montréal, QC H2W 1R7, Canada
[2]Molecular Biology Programs, Université de Montréal, Montréal, QC H3T 1J4, Canada
[3]Institute for Research in Immunology and Cancer (IRIC), Université de Montréal, Montréal, QC H3C 3J7, Canada
[4]Rosalind and Morris Goodman Cancer Research Centre, McGill University, Montréal, QC H3A 1A1, Canada
[5]Laboratory of Angiogenesis and Vascular Metabolism, VIB Vesalius Research Center, VIB, Leuven 3000, Belgium
[6]Laboratory of Angiogenesis and Vascular Metabolism, Department of Oncology, University of Leuven, Leuven 3000, Belgium
[7]Department of Oncology and Surgery, Segal Cancer Center, Lady Davis Institute for Medical Research, Sir Mortimer B. Davis Jewish General Hospital, McGill University, Montréal, QC H3T 1E2, Canada
[8]Department of Pathology and Cell Biology, Université de Montréal, Montréal, QC H3C 3J7, Canada
[9]Department of Pharmacology and Physiology, Université de Montréal, Montréal, QC H3C 3J7, Canada
[10]Department of Biochemistry and Molecular Medicine, Université de Montréal, Montréal, QC H3C 3J7, Canada
[11]Department of Anatomy and Cell Biology, McGill University, Montréal, QC H3A 0C7, Canada
[12]Lead Contact
*Correspondence: jean-francois.cote@ircm.qc.ca
https://doi.org/10.1016/j.celrep.2018.04.019

SUMMARY

AXL is activated by its ligand GAS6 and is expressed in triple-negative breast cancer cells. In the current study, we report AXL expression in HER2-positive (HER2$^+$) breast cancers where it correlates with poor patient survival. Using murine models of HER2$^+$ breast cancer, Axl, but not its ligand Gas6, was found to be essential for metastasis. We determined that AXL is required for intravasation, extravasation, and growth at the metastatic site. We found that AXL is expressed in HER2$^+$ cancers displaying epithelial-to-mesenchymal transition (EMT) signatures where it contributes to sustain EMT. Interfering with AXL in a patient-derived xenograft (PDX) impaired transforming growth factor β (TGF-β)-induced cell invasion. Last, pharmacological inhibition of AXL specifically decreased the metastatic burden of mice developing HER2$^+$ breast cancer. Our data identify AXL as a potential anti-metastatic co-therapeutic target for the treatment of HER2$^+$ breast cancers.

INTRODUCTION

Metastasis is a complex multistep process that involves intra-tumoral cell invasion followed by entry into the circulation (intravasation), and completes when the cancer cells invade (extravasation) and survive in distant tissues to grow as macro-metastatic lesions (Lambert et al., 2017). Unfortunately, once the disease spreads to secondary organs it becomes virtually incurable (Kedrin et al., 2007). Among breast cancers, both the Triple-Negative (TNBC) and HER2-positive (HER2$^+$) subtypes are linked to poor survival due to their propensity for metastasis (Seal and Chia, 2010; Visvader, 2009). HER2 is a member of the epidermal growth factor receptor (EGFR) of receptor tyrosine kinases (RTKs) that is overexpressed or amplified in ~20% of human breast cancers and transmits signals mediating tumor growth, invasion, and metastasis (Brenton et al., 2005). While some patients afflicted with HER2$^+$ breast cancer benefit from anti-HER2 therapeutic treatment, others may either be unresponsive or will develop resistance and relapse with a metastatic disease (De Laurentiis et al., 2005; Mukohara, 2011). Hence, defining the molecular mechanisms by which HER2 promotes cancer spreading may reveal novel anti-metastatic therapeutic strategies.

AXL, TYRO3, and MER collectively form the TAM family of RTKs. Within this family, AXL is specifically activated by its ligand GAS6 (Graham et al., 2014; Linger et al., 2008; O'Bryan et al., 1991). While TAMs are dispensable for embryonic development, their compound genetic deletions in mice revealed their essential role in inhibiting innate immunity (Lemke and Rothlin, 2008; Rothlin et al., 2007). TAMs are frequently implicated in diseases, and AXL is broadly expressed in solid cancers including breast cancer, non-small cell lung carcinoma, ovarian cancer, and clear cell renal carcinoma where its levels correlate with increased risks of metastasis (Gjerdrum et al., 2010; Lozneanu et al., 2016; Rankin et al., 2010; Shieh et al., 2005; Yu et al., 2015). In addition, AXL expression correlates with the acquisition of mesenchymal features of cancer cells and provides advantages to tumors such as increased invasion and resistance to antimitotic agents *in vitro* (Asiedu et al., 2014; Gjerdrum et al., 2010; Vuoriluoto et al., 2011; Wilson et al., 2014). Within breast cancer cell lines, AXL expression is restricted to cells with the Triple-Negative

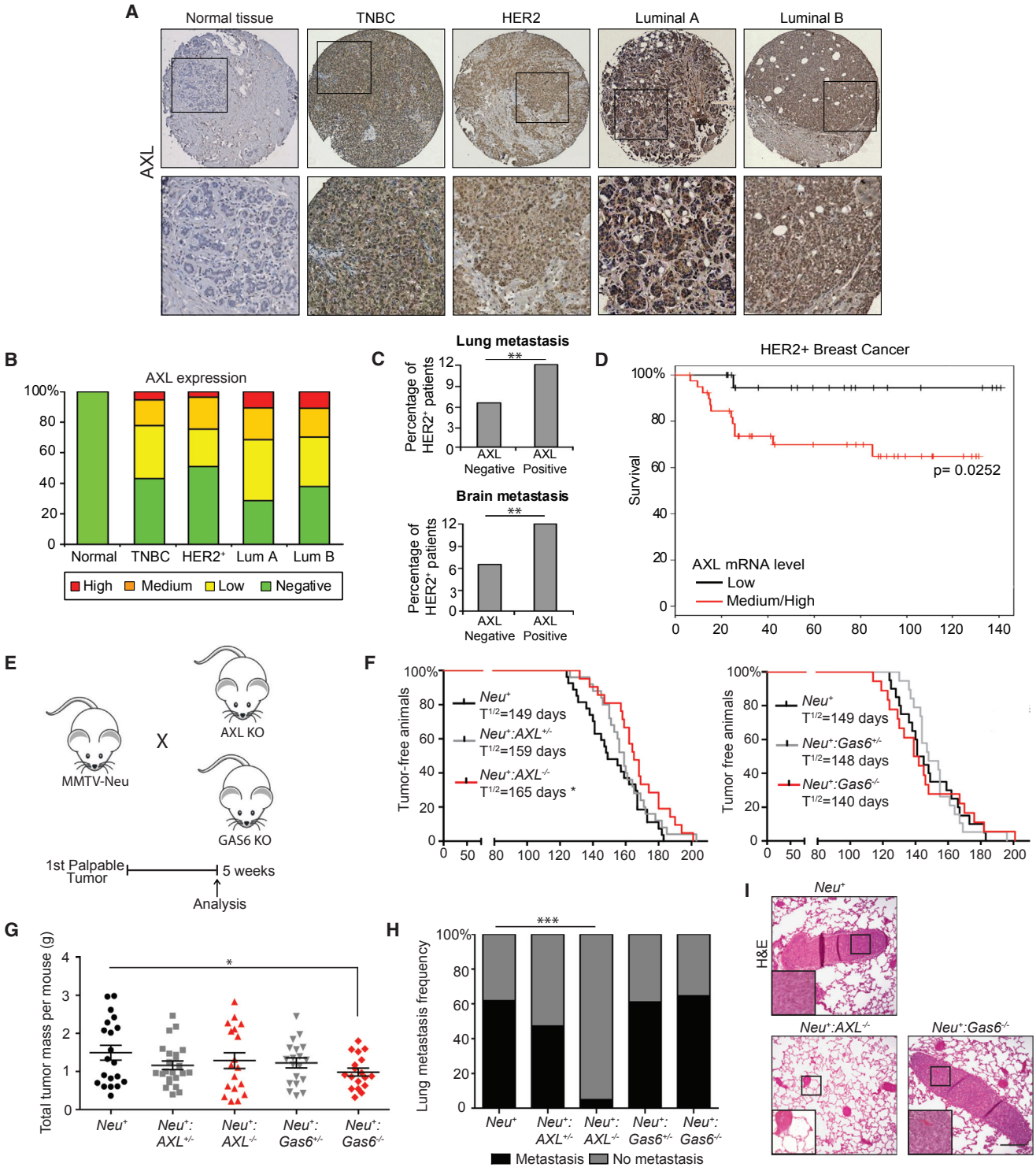

Figure 1. AXL Contributes to Metastasis in Human HER2+ Breast Cancers and in a Mouse Model of the HER2 Subtype

(A and B) TMA staining (A) reveals that AXL is expressed in all breast cancer molecular subtypes (B). Normal mammary gland (n = 10), TNBC (n = 130), HER2+ (n = 57), luminal A (n = 150), luminal B (n = 58).

(C) AXL expression is associated with metastasis in HER2+ breast cancer. TMA staining, AXL negative (n = 16), and AXL positive (n = 17) because not all patients from (A) were followed for metastasis. **p = 0.003.

(D) mRNA level of AXL correlates with overall survival in HER2+ breast cancer samples from GSE58644 (n = 66).

(legend continued on next page)

gene signature, such that AXL is viewed as a marker of this breast cancer subtype (D'Alfonso et al., 2014; Wilson et al., 2014). Whether AXL is activated by GAS6 during cancer progression and metastasis remains unclear. *GAS6* expression correlates with positive outcome in breast cancer (Mc Cormack et al., 2008) while it is linked to increased metastasis in non-small cell lung cancer (Wu et al., 2017). AXL can also bypass the need of GAS6 by cooperating with other transmembrane receptors including EGFR, MET, platelet-derived growth factor (PDGF), and VEGFR-2 (Meyer et al., 2013; Ruan and Kazlauskas, 2012; Salian-Mehta et al., 2013). In this study, we set out to develop murine genetic models of AXL and GAS6 deletion to test their role on metastasis in HER2$^+$ breast cancer. We extended these observations in tumor specimens and human cell lines, including patient-derived xenografts (PDXs), and tested whether pharmacological inhibition of AXL could be a valid strategy to limit breast cancer metastasis.

RESULTS

AXL Expression in HER2$^+$ Breast Cancers Correlates with Poor Patient Outcome

Because expression of AXL in human breast cancer is reported to be limited to cell lines derived from TNBC patients (D'Alfonso et al., 2014), AXL is currently viewed as a marker of the TNBC molecular subtype (Leconet et al., 2016). Indeed, analysis of RNA sequencing (RNA-seq) data (Wilson et al., 2014) revealed that only TNBC cell lines express high levels of *AXL* and this is correlated with *Vimentin* (*VIM*) expression, suggesting that AXL is expressed in cell lines displaying mesenchymal features (Figure S1A). However, analyses of the expression levels of AXL in breast cancer patient samples has yielded conflicting data for expression in molecular subtypes and for patient outcomes (Gjerdrum et al., 2010; Jin et al., 2017; Wilson et al., 2014; Wu et al., 2015). To resolve which breast cancer molecular subtypes express AXL at the protein level, we stained a panel of tumor microarrays (TMA) (Yousef et al., 2014), derived from breast tumor specimens linked with clinical data, using an AXL antibody that had been validated for immunostaining on human samples (Wilson et al., 2014) and that we validated in this study (Figure S1B). Unlike observations made in cell lines, these analyses revealed that AXL expression was broadly detectable across breast cancer subtypes (Figures 1A and 1B). Furthermore, high expression of AXL protein correlated with adverse clinical outcome when data from all breast cancer subtypes were pooled (Figure S1C). We sought to characterize the role of AXL in HER2$^+$ breast cancers because this molecular subtype is aggressive and prone to progress to a metastatic disease. We found that high AXL protein levels correlated with lung and brain metastases in HER2$^+$ patients (Figure 1C). We analyzed transcriptomics data linked to clinical data of our cohort of HER2$^+$ breast cancer patients (GSE58644) and found that low expression of *AXL* correlated with better survival (Figure 1D). Thus, high AXL expression in HER2$^+$ breast cancer unexpectedly correlates with increased risk of metastasis and a reduced probability of survival.

Axl Promotes the Metastatic Progression of HER2$^+$ Breast Cancer *In Vivo* Independently of Gas6

Because we found that AXL expression correlated with poor outcome of HER2$^+$ breast cancer patients, we used a murine HER2$^+$ breast cancer model to investigate the specific contributions of AXL and its ligand GAS6 in disease progression. Expression of a deletion mutant of the rat ortholog of HER2 targeted to the mammary gland of mice using mouse mammary tumor virus promoter (MMTV; NeuNDL2-5) results in tumors that progress to invasive carcinoma and metastasize to lungs (Ursini-Siegel et al., 2008). Transcriptomic data revealed that *Axl* and *Gas6* were both expressed in MMTV-NIC tumors (Laurin et al., 2013), suggesting that this model would be useful to determine their functions *in vivo* during HER2-driven breast cancer progression. After verifying that mammary gland development occurred normally in the absence of *Axl* or *Gas6* (Figures S2A–S2C), we interbred *Axl* and *Gas6* germline knockout mice with MMTV-Neu animals to generate five female cohorts: *Neu*$^+$, *Neu*$^+$*:Axl*$^{+/-}$, *Neu*$^+$*:Axl*$^{-/-}$, *Neu*$^+$*:Gas6*$^{+/-}$, and *Neu*$^+$*:Gas6*$^{-/-}$ (Figure 1E). We reasoned that these Axl and Gas6 knockout models would faithfully mimic an effective systemic inhibition of this ligand/RTK pair. The mice were monitored by weekly palpation to test for apparition of tumors. We found that all genotypes developed mammary tumors and noted a minor delay of tumor onset for *Neu*$^+$*:Axl*$^{-/-}$ females, whereas *Neu*$^+$*:Gas6*$^{-/-}$ mice presented no difference as compared to the *Neu*$^+$ control (Figure 1F). Five weeks after tumor onset, the mice were sacrificed for characterization of tumor initiation, tumor growth, and metastasis. To characterize the tumor initiation process, we quantified the number of mammary intraepithelial neoplastic lesions (MINs) on inguinal mammary glands. Only *Neu*$^+$*:Axl*$^{-/-}$ females presented an increased number of MINs suggesting that neoplastic initiation occurs efficiently in the absence of *Axl* (Figures S2D and S2E). Furthermore, all genotypes bore tumors with a solid adenocarcinoma phenotype (confirmed by a pathologist) suggesting that loss of *Axl* or *Gas6* did not alter the differentiation state of the tumors (Figure S2F). While loss of *Axl* did not alter the total tumor mass, a small decrease was observed when *Gas6* was ablated (Figure 1G). To assess the proliferative and apoptotic status of the tumors, we stained them for Ki67 or cleaved-caspase 3, respectively, and while we found no difference in proliferation or apoptosis in Axl null tumors, tumors devoid of Gas6 showed increased apoptosis (Figures S2G–S2I). This increase in apoptosis was independently confirmed by TUNEL staining and likely explained the decrease in tumor mass seen in Gas6 mutants (Figures S2J and S2K). Strikingly, *Neu*$^+$*:Axl*$^{-/-}$ mice

(E) MMTV-Neu mice were crossed with AXL KO or GAS6 KO mice and the cohort was analyzed 5 weeks after tumor onset.
(F) Kaplan-Meier analyses of tumor onset (n = 20–23). *p = 0.015.
(G) Axl does not contribute to HER2-induced tumor growth, but *Neu*$^+$*:Gas6*$^{-/-}$ mice show a reduction of total tumor mass (n = 20). *p = 0.0314.
(H and I) *Neu*$^+$*:Axl*$^{-/-}$ mice were protected from lung metastasis (H) (n = 20–23). ***p = 0.0006 (Chi-square analysis). Representative images (I) (10×). Scale bar, 250 μm.
See also Figures S1 and S2 and Table S2.

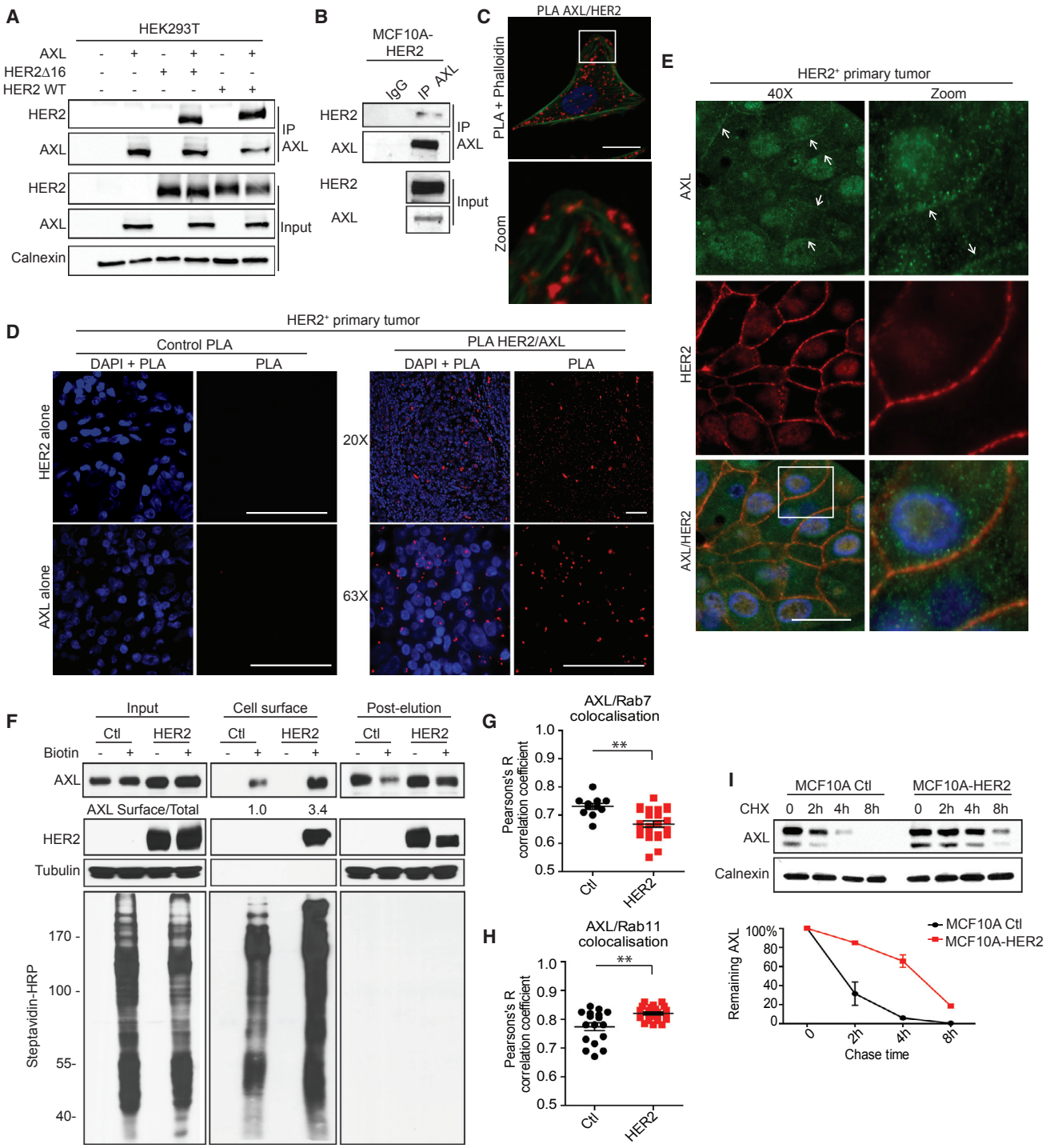

Figure 2. HER2 Interacts with AXL to Promote Its Stability and Accumulation at the Cell Surface

(A and B) AXL co-immunoprecipitates with HER2 WT and Δ16 when co-overexpressed in HEK293T (A) and MCF10A stably expressing HER2 (B). MCF10A-HER2 cells were treated with the DSP chemical crosslinker to detect the interaction.

(C) Proximity ligation assay (PLA) confirms AXL and HER2 interaction in MCF10A-HER2 cells. Scale bar, 20 μm.

(D) PLA shows that AXL and HER2 are found as heterodimers in primary human HER2 tumors (representative images of n = 4 tumors). Scale bar, 50 μm.

(E) AXL and HER2 colocalizes at the cell surface in human samples (representative images of n = 4 tumors). Scale bar, 25 μm.

(F) Surface biotinylation assays show that AXL is enriched at the cells surface in HER2 expressing cells (normalized intensity). *p = 0.0394. See also Figures S3E and S3F.

(legend continued on next page)

exhibited a decrease in both the frequency and the total number of lung metastatic lesions (Figures 1H, 1I, and S2L). In contrast, ablation of *Gas6* had no effect on the lung metastatic burden (Figures 1H, 1I, and S2L). These data demonstrate an essential and Gas6-independent contribution of Axl to the metastatic progression of HER2$^+$ breast cancer.

HER2 Complexes with AXL to Promote Its Stability and Recruitment at the Cell Surface

Because our mouse models revealed that Gas6 is dispensable for the metastatic progression of HER2$^+$ breast cancer, we investigated the possibility of crosstalk between AXL and HER2. We tested if AXL can co-immunoprecipitate with either human HER2 or its splice variant HER2 Δ16 that is frequently expressed in human tumors (Kwong and Hung, 1998; Siegel et al., 1999). An interaction between AXL and HER2 and HER2 Δ16 was detected when the proteins were co-expressed in HEK293T cells (Figure 2A). The interaction between AXL and HER2 was also detectable both by co-immunoprecipitation and proximity ligation assay (PLA) in MCF10A cells that stably express HER2 (Figures 2B and 2C). Furthermore, immunofluorescence revealed that the AXL/HER2 complex is localized at cell edges in MCF10A-HER2 cells (Figures 2C and S3A). An interaction between endogenous HER2 and AXL was also detectable in SKBR3 cells (Figure S3B). Because all of the mouse models and mouse cell lines used in this study exploit either NeuNDL2-5 or an activated mutant of Neu (NeuT; V664E mutant), we tested whether these variants also interact with AXL. We found that AXL co-precipitated with NeuT not only when the proteins were co-expressed in HEK293T cells, but also endogenously with NeuNDL2-5 in NIC cells (a cell line derived from the MMTV-Neu-IRES-Cre mice) (Ursini-Siegel et al., 2008) (Figures S3C and S3D). To test whether AXL was also found in a complex with HER2 in tumors from HER2$^+$ breast cancer patients, we performed PLA experiments that revealed the existence of AXL/HER2 complexes in human tumors (Figure 2D). In addition, immuno-staining for both proteins revealed that a pool of AXL is co-localized with HER2 at the plasma membrane in HER2$^+$ tumor samples (Figure 2E).

To address the functional impact of HER2/AXL coupling, we performed surface biotinylation experiments in MCF10A control and MCF10A-HER2 cells to determine AXL protein levels at the cell surface. These experiments revealed that HER2 expression leads to a 3.4-fold increase in the cell surface pool of AXL, and this enrichment occurs despite a decrease in the expression of *AXL* and *GAS6* at the mRNA levels (Figures 2F and S3E). Interestingly, this HER2-mediated enrichment of AXL at the cell surface was not dependent on the kinase activity of either AXL or HER2 (Figure S3F). One possible explanation for the HER2-associated increase in AXL at the cell surface is that HER2 affects the trafficking of AXL and we therefore tested the localization of AXL with late (Rab7$^+$) or recycling (Rab11$^+$) endosomes. Using an AXL antibody that stained the intracellular pool of AXL, these experiments revealed that in cells expressing HER2, the presence of AXL decreased in Rab7$^+$ late endosomes and increased in Rab11$^+$ recycling vesicles as compared to the control cells (Figures 2G, 2H, S3G, and S3H). To test whether the coupling of AXL to HER2 might stabilize the protein, we performed cycloheximide chase assays that revealed that the AXL protein is more stable in MCF10A-HER2 ($t_{1/2}$ = 5.13 hr) than in the control MCF10A cells ($t_{1/2}$ = 1.73 hr) (Figure 2I). Collectively, these results suggest that AXL and HER2 form a physical complex that lead to HER2-mediated stabilization of AXL and its enrichment at the cell surface.

HER2 Transphosphorylates AXL to Promote Cancer Cell Invasion

Because a proteomic screen of HER2 overexpression revealed AXL as a candidate substrate (Bose et al., 2006), we hypothesized that the formation of an AXL/HER2 complex might facilitate transphosphorylation events between these RTKs. To test this, we overexpressed the human HER2 Δ16 or NeuT together with a kinase dead (KD) mutant of AXL in HEK293T cells. These experiments revealed that both HER2 Δ16 and NeuT phosphorylate AXL KD in a HER2 kinase activity-dependent manner because it was sensitive to the HER2 inhibitor lapatinib (Figures 3A and S4A). We next expressed HER2 Δ16 or NeuT in MDA-MB-231 cells that express endogenous HER2 at very low levels and AXL at high levels. We found that oncogenic HER2 variants promoted the phosphorylation of endogenous AXL, and these events were abrogated by inhibiting HER2 activity with lapatinib (Figures 3B and S4B). We also tested whether AXL could promote the phosphorylation of HER2 in T47D luminal A cells, which expresses HER2 but not AXL. In these cells, expression of exogenous AXL, which was found to be phosphorylated at basal state, had no impact on HER2 phosphorylation (Figure 3C). Similarly, inhibition of AXL with the small molecule inhibitor R428 in the MCF10A-HER2, NIC, and SKBR3 cell lines had no impact on the phosphorylation of HER2 on multiple tyrosine sites (Figure S4C). Interestingly, in T47D overexpressing AXL, addition of lapatinib was sufficient to decrease AXL phosphorylation (Figure 3C), and this effect could be reproduced with MCF10A-HER2, NIC, and SKBR3 cell lines (Figure S4E). We also found that treatment of T47D cells with heregulin (HRG), a ligand of the HER2/HER3 heterodimer, led to a further increase in AXL phosphorylation (Figure 3C). We confirmed that lapatinib, at the concentration used here (0.1–1 μM), showed no off-target activity on AXL in a GAS6-mediated activation of AXL (Figure S4D). We subsequently investigated whether the co-inhibition of HER2 and AXL would have a functional impact on cell invasion. While treatments with the HER2 blocking agents lapatinib or herceptin (antibody) had no impact, the AXL inhibitor R428 was sufficient to reduce cell invasion in MCF10A-HER2, SKBR3, and NIC cells (Figures 3D–3G, S4F, and S4G). However,

(G and H) AXL is less present in late endosomes (Rab7$^+$) (G) and enriched in recycling vesicles (Rab11$^+$) (H) in MCF10A-HER2 cells. See also Figures S3G and S3H (n = 15–25 cells). **p = 0.0013, **p = 0.0061.

(I) Cycloheximide (CHX) chase shows that AXL stability is increased in MCF10A-HER2 cells in comparison to control cells. ***p < 0.0001.

See also Figure S3.

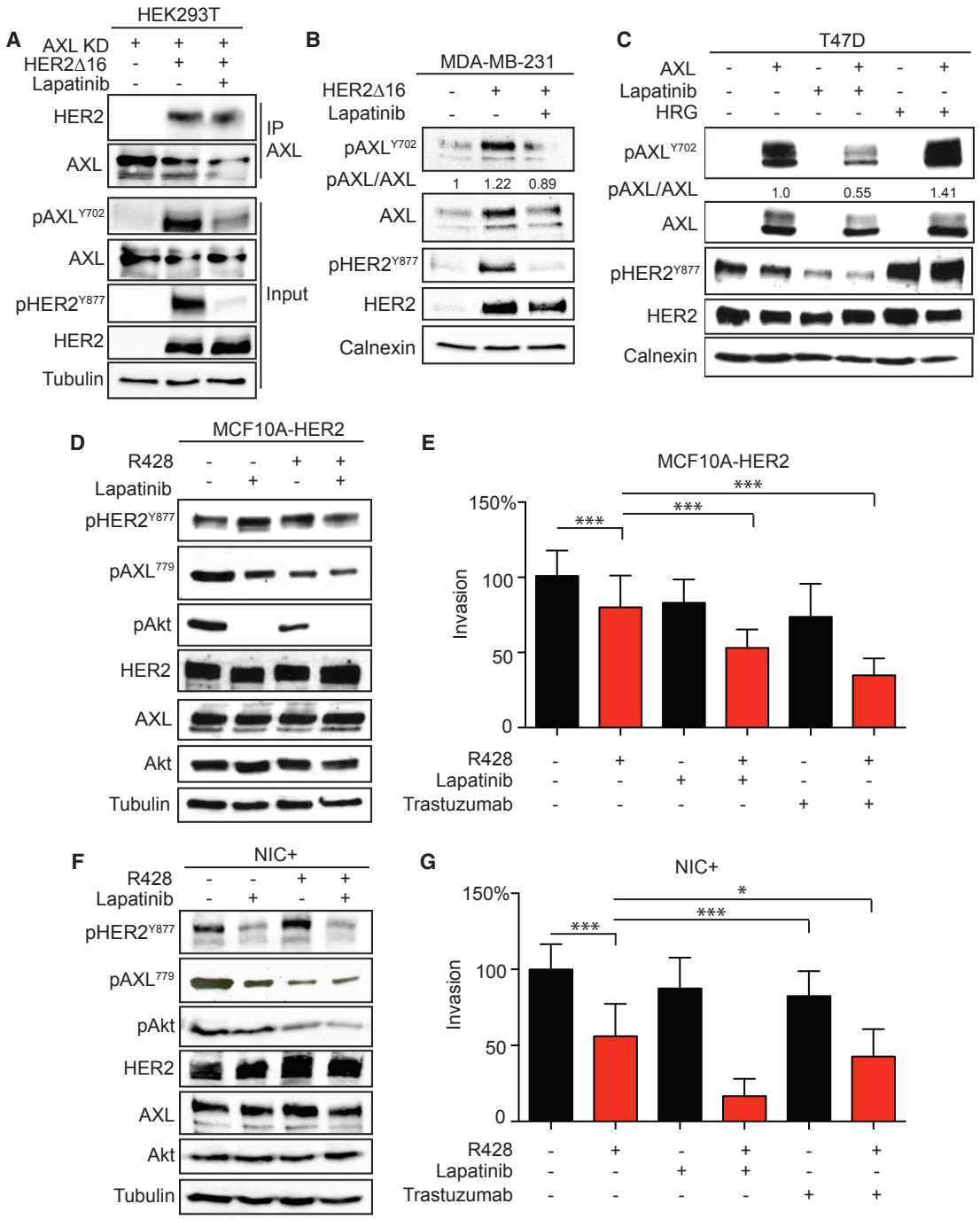

Figure 3. HER2 Transactivates AXL to Promote Cell Invasion

(A) Overexpression of HER2Δ16 promotes the phosphorylation of AXL (kinase dead) and this is blocked by the HER2 inhibitor lapatinib (1 μM).

(B) Expression of HER2Δ16 in MDA-MB-231 cells promotes transactivation of endogenous AXL, which is blocked by lapatinib (1 μM) (n = 3). *p = 0.049.

(C) Expression of AXL in serum-starved T47D cells does not promote transactivation of endogenous HER2, but activation or inhibition of HER2 modulates AXL phosphorylation (n = 3). Lapatinib (1 μM) **p = 0.002 and HRG (20 ng/mL) 20 min, **p = <0.0074.

(D–G) R428 (1 μm) and lapatinib (1 μM) or trastuzumab (10 μg/mL) cooperates to decrease MCF10A-HER2 (D and E) and NIC (F and G) cell invasion. Data are represented as mean ± SEM, *p = 0.0117 and ***p < 0.0001.

See also Figure S4.

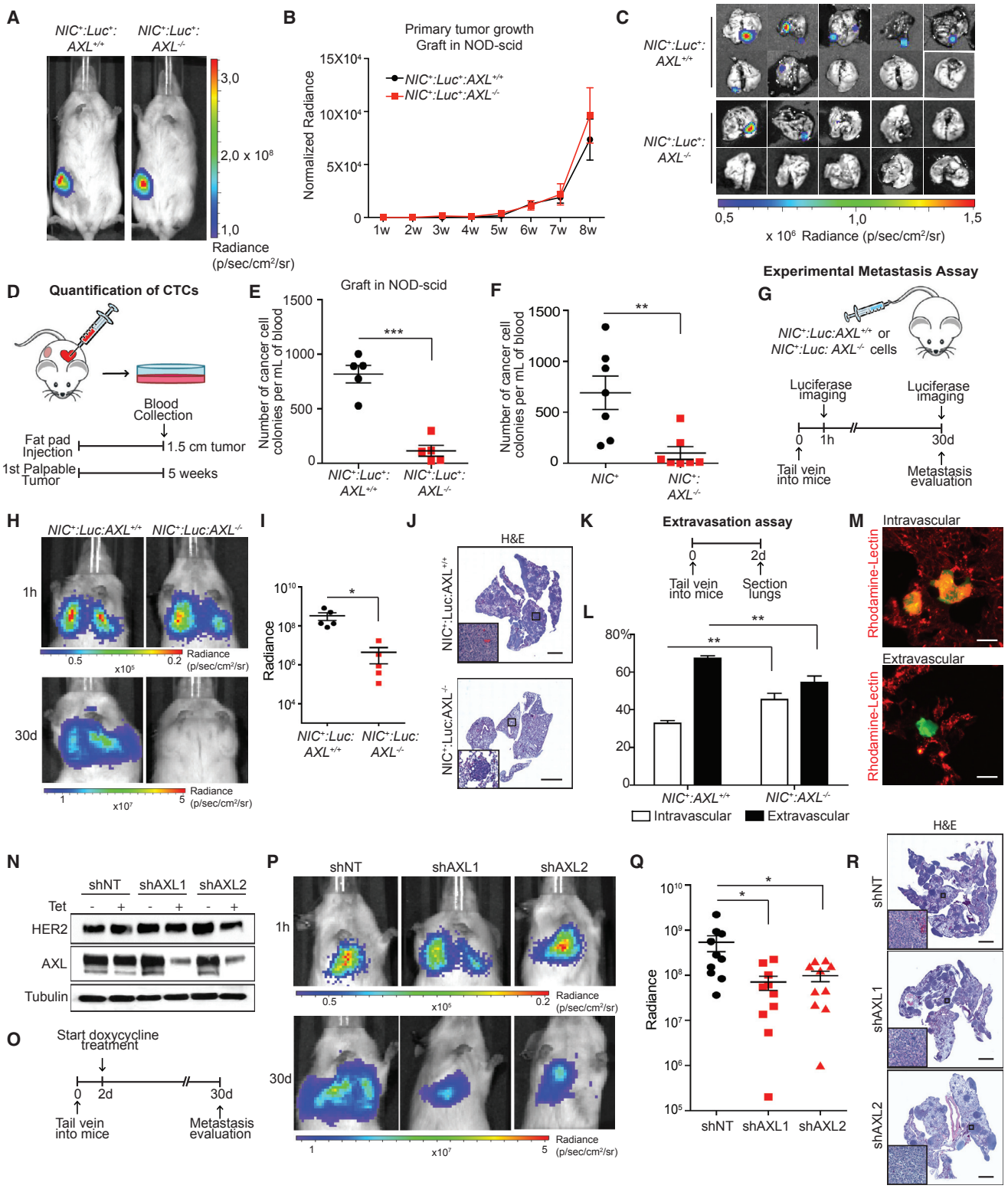

Figure 4. AXL Is Required at Multiple Steps of the Metastatic Cascade

(A–C) *NIC*$^{+}$*:Luc*$^{+}$*:Axl*$^{-/-}$ cells grafted in NOD-SCID mice present no difference in tumor growth (A and B), but developed less lung metastases (C) (n = 10). (D) Schematic showing the method for quantifying the circulating tumor cells (CTCs) as a measure of intravasation.

(legend continued on next page)

co-treatments of lapatinib or trastuzumab together with R428 robustly blocked invasion (Figures 3D–3G, S4F, and S4G). Collectively, these data suggest that HER2 complexes with AXL for its transphosphorylation that promotes cell invasion.

AXL Is Implicated in Multiple Steps of the Metastatic Cascade

The generation of a *Neu*$^{+}$*:Axl*$^{-/-}$ mouse model is the first bona fide pre-clinical tool to dissect the roles of AXL at various steps of the metastatic cascade *in vivo*. One of the potential limitations of the *Neu*$^{+}$*:Axl*$^{-/-}$ mouse model is that the global deletion of AXL might also have an impact on the tumor microenvironment. We therefore reconstituted NOD-SCID immune-compromised mice with control or Axl null breast cancer cells to determine the tumor cell intrinsic role of AXL. We generated two cohorts of mice that conditionally express the Luciferase reporter in mammary epithelial cells: *NIC*$^{+}$*:Rosa Lox-STOP-Lox Luciferase:Axl*$^{+/+}$ or *NIC*$^{+}$*:Rosa Lox-STOP-Lox Luciferase:Axl*$^{-/-}$, and we derived cell explants from these models (*NIC*$^{+}$*:Luc*$^{+}$*:Axl*$^{+/+}$ and *NIC*$^{+}$*:Luc*$^{+}$*:Axl*$^{-/-}$). When injected in mammary fat pads of NOD-SCID mice, *NIC*$^{+}$*:Luc*$^{+}$*:Axl*$^{-/-}$ cells grew as primary tumors as efficiently as the control cells (Figures 4A and 4B). Furthermore, at endpoint, 2/10 mice grafted with *NIC*$^{+}$*:Luc*$^{+}$*:Axl*$^{-/-}$ cells showed lung metastasis while 7/10 mice grafted with the control cells developed metastases (Figure 4C). These results demonstrate that AXL expressed in the HER2 transformed mammary epithelial cells promotes metastasis but is dispensable for tumor growth.

We next investigated the contribution of AXL in cancer cells at different steps of the metastatic cascade including intravasation, extravasation, and survival/growth at the metastatic site. To assess the potential of AXL to promote intravasation, we implanted *NIC*$^{+}$*:Luc*$^{+}$*:Axl*$^{+/+}$ or *NIC*$^{+}$*:Luc*$^{+}$*:Axl*$^{-/-}$ cells in mammary fat pads of NOD-SCID mice and quantified the circulating tumor cells (CTCs) when the primary tumors had reached a 1.5 cm diameter (Figure 4D). We also quantified the CTCs directly from the *NIC*$^{+}$ and *NIC*$^{+}$*:Axl*$^{-/-}$ transgenic models 5 weeks after tumor onset (Figure 4D). NOD-SCID mice bearing *NIC*$^{+}$*:Luc*$^{+}$*:Axl*$^{-/-}$ tumors as well as *NIC*$^{+}$*:Axl*$^{-/-}$ transgenic mice presented with only a few CTCs in comparison to their respective control animals (Figures 4E and 4F). These results suggest that the AXL protein is a major contributor of intravasation.

We subsequently conducted an experimental metastasis assay by injecting *NIC*$^{+}$*:Luc*$^{+}$*:Axl*$^{+/+}$ or *NIC*$^{+}$*:Luc*$^{+}$*:Axl*$^{-/-}$ cells directly in the lateral tail vein of NOD-SCID mice, therefore bypassing the intravasation process (Figure 4G). While both cell models were retained in the lungs 1 hr post-injection, *Axl*$^{-/-}$ cells produced noticeably less metastatic lesions than the control cells 30 days post-injection (Figures 4H–4J). We designed an assay to specifically measure the extravasation potential of *Axl* null cells by injecting fluorescently stained *NIC*$^{+}$*:Luc*$^{+}$*:Axl*$^{+/+}$ or *NIC*$^{+}$*:Luc*$^{+}$*:Axl*$^{-/-}$ cells in the lateral tail vein of NOD-SCID mice. Two days later, Rhodamine-labeled lectin was injected to stain the blood vessels and lungs were collected and sectioned to measure the ability of cells to enter the lung tissue (Figure 4K). These experiments revealed a decreased ability of Axl null cells to exit the blood vessels and invade into the lung parenchyma (Figure 4L-M). To test whether AXL is also required in the cancer cells to promote survival and growth at the metastatic site, we developed a conditional AXL-depletion assay by generating *NIC*$^{+}$*:Luc*$^{+}$ cells stably expressing 2 independent and Tet-inducible small hairpin RNAs (shRNAs) against *Axl* (Figure 4N). We performed an experimental metastasis assay and waited for 2 days for the cells to extravasate into the lungs prior to treating the mice with doxycycline for 28 days to induce *Axl* knockdowns (Figure 4O). Cells in which Axl was conditionally depleted grew significantly less at the metastatic site than the ones expressing a non-targeting shRNA (Figures 4P and 4R). Collectively, these data suggest that AXL is continuously required in HER2^{+} cancer cells for efficient metastasis.

AXL Regulates Transforming Growth Factor β-Induced Cell Invasion of HER2^{+} Breast Cancer Cells

To gain mechanistic insights into the poor metastatic potential of *Axl* null tumors, we performed a transcriptomic analysis. We first conducted RNA-sequencing experiments using RNA isolated from *Neu*$^{+}$*:Axl*$^{+/+}$ or *Neu*$^{+}$*:Axl*$^{-/-}$ tumors grown as grafts and identified the differentially expressed genes. Gene Ontology analysis revealed that *Axl*$^{-/-}$ tumors displayed a decrease in expression of genes involved in pathways mediating Integrin, EGF, Rho-GTPase, and transforming growth factor β (TGF-β) signaling (Figure 5A) as compared to *Axl*-expressing tumors. These analyses also identified biological processes downregulated following the loss of AXL, including extracellular matrix organization, cell migration, cytoskeleton organization, and epithelial-to-mesenchymal transition (EMT) (Figure 5B). Furthermore, gene set enrichment analysis (GSEA) suggested that AXL acts on TGF-β signaling, EMT, and cell migration (Figures 5C, and 5D; Table S1). Additionally, gene sets from focal adhesion, stem cell, and HER2 signaling were also decreased in *Axl*$^{-/-}$ tumor grafts (Figures S5A–S5D). Similar GSEA signatures were

(E and F) *NIC*$^{+}$*:Luc*$^{+}$*:Axl*$^{-/-}$grafts in NOD-SCID (E) and *NIC*$^{+}$*:Axl*$^{-/-}$ (F) mice have a decrease in the number of CTCs. Data are represented as mean ± SEM (n = 5–7). **p = 0.0057, ***p < 0.0001.

(G) Schematic showing the experimental metastasis assay via lateral tail vein injection of the cells.

(H–J) *NIC*$^{+}$*:Luc*$^{+}$*:Axl*$^{-/-}$cells have a reduced metastatic potential in experimental metastasis assay (H and I) (n = 5, *p = 0.0487). Representative H&E staining of metastatic lung sections (J). Scale bar, 2 mm.

(K) Representation of an *in vivo* lung extravasation assay via lateral tail vein injection of the cells.

(L and M) *NIC*$^{+}$*:Luc*$^{+}$*:Axl*$^{-/-}$ cells have a defect in extravasation to the lung (L) (n = 5 mice, 20–30 cells per lung). **p = 0.0085 and **p = 0.0071. Representative images of intravascular and extravascular cells quantified in the lung (M) (63×). Scale bar, 20 μm.

(N) Western blot showing the efficiency of tetracycline-mediated induction of the two shAxl in *NIC*$^{+}$*:Luc*$^{+}$ cells.

(O) Schematic of the experimental metastasis assay with doxycycline treatment setting for the induction of the shRNA *in vivo*.

(P–R) Induction of *Axl* knockdown after extravasation in the lung leads to a decrease of metastatic burden (P and Q) (n = 10). *p = 0.0386, *p = 0.0497. Representative H&E staining of metastatic lung sections (R). Scale bar, 2 mm.

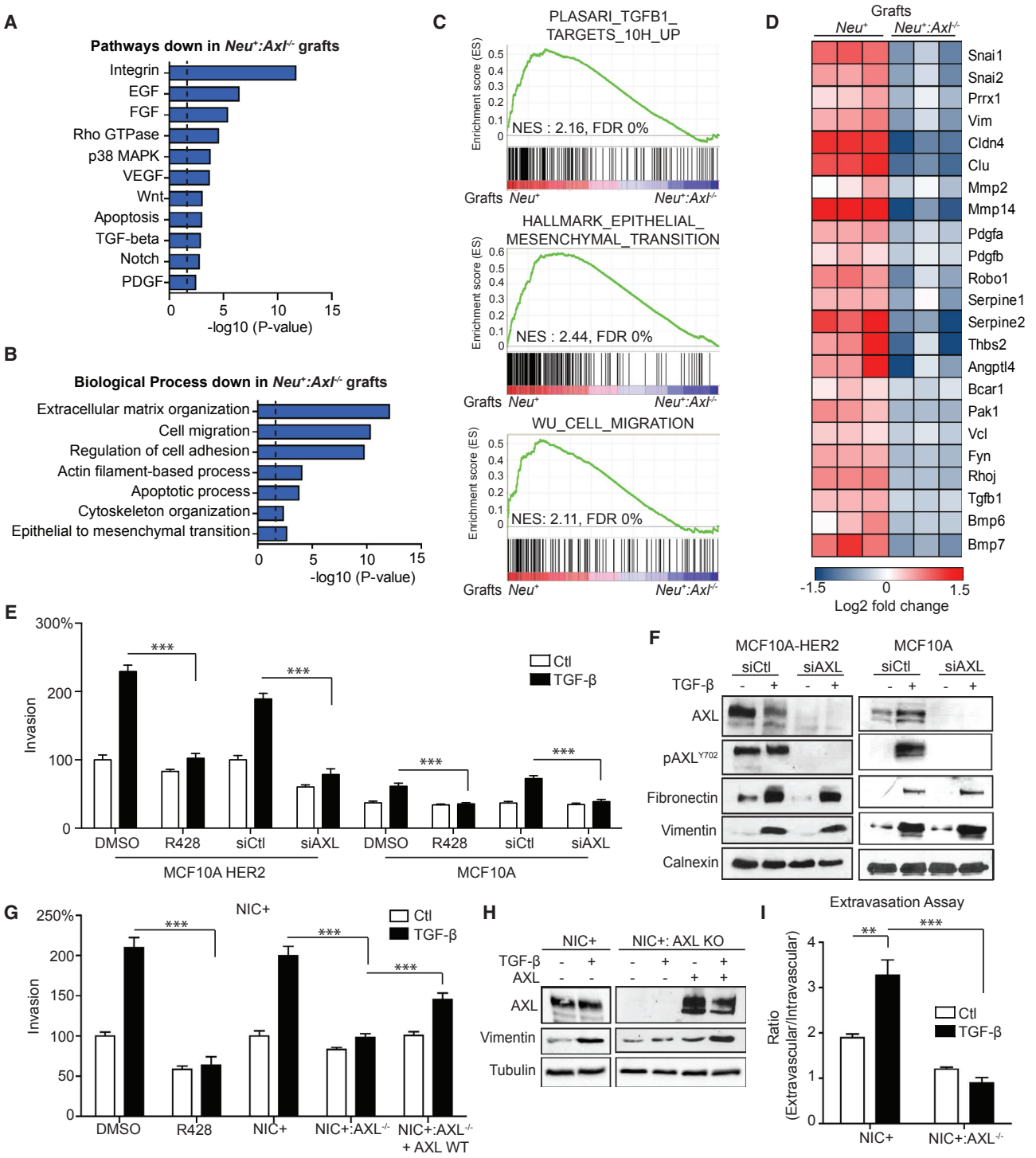

Figure 5. Transcriptomics Analyses Reveal a Role for AXL in TGF-β and EMT Signaling

(A and B) Gene ontology (GO) analyses of pathways (A) and biological processes (B) downregulated in Axl null tumor grafts in FVB females.

(C and D) GSEA plots (C) and heatmaps (D) representing significant modulated genes related to TGF-β signaling, EMT, and cell migration between $Axl^{-/-}$ and control tumor grafts. See also Figure S5.

(E and F) AXL is essential for TGF-β-induced cell invasion of MCF10A-HER2 (***$p < 0.0001$) and control MCF10A cells treated with TGF-β (E) (***$p < 0.0001$). Validation of protein knockdowns and EMT-induction is shown in (F).

(legend continued on next page)

identified when RNA was isolated from tumors from *Neu*$^{+}$*:Axl*$^{+/+}$ or *Neu*$^{+}$*:Axl*$^{-/-}$ transgenic mice (Figures S5E–S5H; Table S1). These analyses suggest that AXL may promote metastasis by controlling cell migration and invasion in the context of EMT/TGF-β signaling. We investigated the activation status of a panel of proteins involved in cell migration using activation state-specific antibodies. Tissue lysates from *Neu*$^{+}$*:Axl*$^{-/-}$ tumors displayed a reduction of pSrc, pFAK, p-p130Cas, and pAKT suggesting that migration pathways are impaired when AXL is absent (Figure S5I). Interestingly, ablation of *Gas6* had no impact on the activation status of these pro-migration proteins (Figure S5I). Other signaling intermediates, pSTAT3, pSTAT1, or pERK, were unaffected by deletion of *Axl* or *Gas6* (Figure S5I).

Previous work has shown that TGF-β promotes the formation of metastases *in vivo* in *Neu*$^{+}$ breast cancer models (Siegel et al., 2003), and the plasticity of EMT is important for efficient metastasis (Lambert et al., 2017; Li and Kang, 2016; Aceto et al., 2015; Tsai and Yang, 2013). Because our transcriptomics experiments indicated that deletion of AXL in *Neu*$^{+}$ tumors alters their EMT status, we hypothesized that AXL is required to promote EMT-induced cell migration and invasion. To test this, we exposed a panel of HER2^{+} breast cancer cell models (NIC, MCF10A-HER2, and SKBR3) to TGF-β to reprogram them toward EMT. As expected, TGF-β stimulation increased cell invasion, which could be blunted either by treatment with R428, by interfering with AXL expression using either RNAi or genetic knockout (Figures 5E–5H and S6A–S6L; Video S1). Treatment of the non-transformed MCF10A cells with TGF-β increased AXL expression, its phosphorylation, the expression of EMT markers, and increased cell migration and invasion (Figures 5E, 5F, S6C, and S6D). In this model, interfering with AXL activity (R428) or expression (small interfering RNA [siRNA]) abolished TGF-β-induced cell migration and invasion and this effect was more striking in MCF10A-HER2 in comparison to MCF10A cells (Figures 5E, 5F, and S6A–S6D). Furthermore, TGF-β failed to induce invasion of *NIC*$^{+}$*:Axl*$^{-/-}$ or *NIC*$^{+}$:shAXL cells, and this phenotype could be rescued by re-expression of AXL (Figures 5G, 5H, S6K, and S6L). To test whether AXL contributes to TGF-β-induced invasion *in vivo*, we conducted an extravasation assay similar to the one described in Figure 4K. While pre-treatment of Neu^{+}:Axl$^{+/+}$ cells enhanced their invasion in the lung, TGF-β had no effect on the extravasation potential of Neu^{+}:Axl$^{-/-}$ *in vivo* (Figure 5I). These results suggest that AXL plays a critical role in EMT/TGF-β-induced cell invasion of HER2^{+} breast cancer cells *in vivo*.

AXL Is a Critical Effector of EMT for Invasion of Human HER2^{+} Breast Cancers

We next investigated whether the EMT/TGF-β/AXL interplay contributes to human HER2^{+} breast cancer progression. Unlike in human tumors (Figure 1), AXL is not significantly expressed in human HER2^{+} breast cancer cell lines (Figure S1A). We used the human HER2^{+} breast cancer cell line HCC1954 and confirmed that AXL expression is increased upon TGF-β treatment (Figures 6A and S7A). In this context, interfering with AXL activity (R428) or expression (siRNA) abolished TGF-β-induced cell migration and invasion (Figures 6A, 6B, and S7A–S7C). We found that AXL expressed following TGF-β treatment of HCC1954 cells enters in complex with HER2 by PLA (Figure 6C). We also observed that AXL phosphorylation is decreased following treatment with lapatinib in TGF-β-treated HCC1954 cells (Figure 6D). While R428 decreased the invasiveness of HCC1954 cells stimulated with TGF-β, the combination of R428 with the HER2 targeting agents lapatinib or trastuzumab further blocked this phenotype (Figure 6E). Furthermore, we derived a cell line from a HER2^{+} PDX initially isolated as a brain metastasis. In agreement with the observations from a panel of human HER2^{+} cell lines, AXL is not expressed in the HER2^{+} PDX cells, but its expression, along with EMT markers, is induced following TGF-β stimulation (Figures 6F and S7D). While TGF-β treatment robustly induced cell invasion and migration of the PDX cells, interfering with AXL activity (R428) or expression (shAXL) blunted these effects (Figures 6F, 6G, and S7D–S7F; Video S2). Interestingly, AXL induced after TGF-β treatment of the PDX-derived cells formed a complex with HER2 (Figure 6H). The combination of R428 with lapatinib or trastuzumab in this context also blocked cell invasion in comparison to each agent alone (Figure 6I).

We next investigated if AXL expression in HER2^{+} breast cancer samples correlates with the EMT status of the tumors and found that AXL expression inversely correlated with the epithelial marker E-Cadherin and correlated with the mesenchymal marker Slug (Figure 6J). To confirm the correlation between *AXL* expression and the EMT status of the tumors, we mined the transcriptomic data of our cohort of HER2^{+} breast cancer patient samples and these analyses demonstrated that high expression of the *AXL* mRNA strongly correlates with TGF-β gene signatures in HER2^{+} tumors (Figure 6K). Immunofluorescence showed cancer cells to be positive for both pSmad2 and AXL (Figure S7G), thereby confirming that this signature is present in the cancer cells, and not only in the stroma. Our results in mouse models and human samples highlight a role for AXL in the maintenance of the EMT program and demonstrate that EMT/TGF-β signaling promotes AXL expression that mediates invasion breast cancer cells.

Pharmacological Inhibition of AXL Reduces the Metastatic Progression of HER2^{+} Breast Cancer

Because our results support a role for AXL in promoting metastasis of HER2^{+} breast cancer, we tested whether pharmacological inhibition of AXL might be a viable anti-metastatic treatment. We used a tumorsphere model in which the ability of cancer cells with stem-like properties to form tumorspheres *in vitro* is a reflection of their capacity to form tumors *de novo* or at the metastatic

(G and H) NIC cells undergo EMT upon treatment with TGF-β and the inhibition of AXL abrogates TGF-β-induced cell invasion (G). TGF-β-induced cell invasion in Axl-depleted cells was rescued with exogenous Axl expression (H). Data are represented as mean ± SEM, ***$p < 0.0001$.
(I) TGF-β-induced cell extravasation *in vivo* is abrogated in *NIC*$^{+}$*:Axl*$^{-/-}$ cells (n = 5 mice). **$p = 0.0036$, ***$p < 0.0001$.
See also Figure S5 and Table S1.

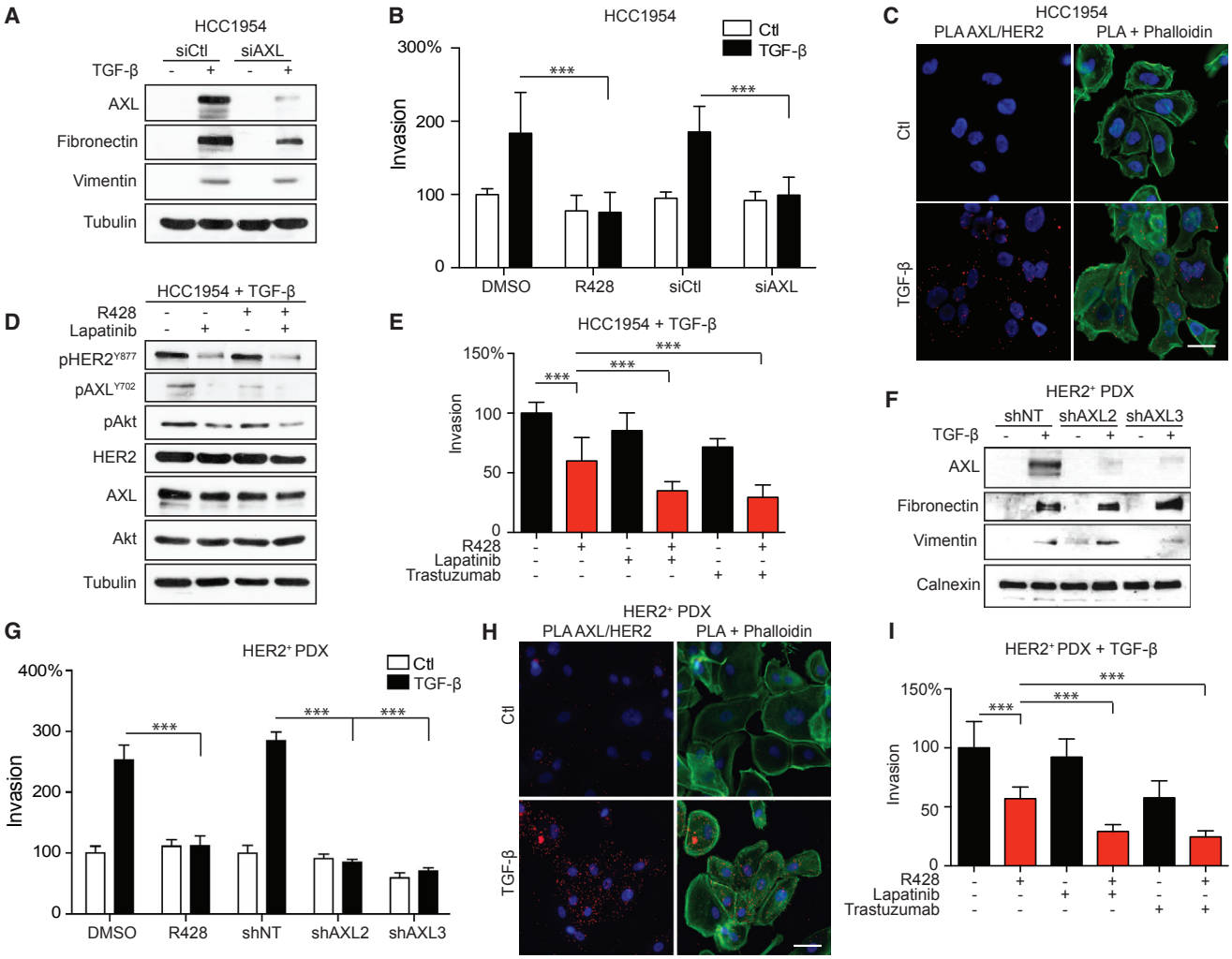

(legend on next page)

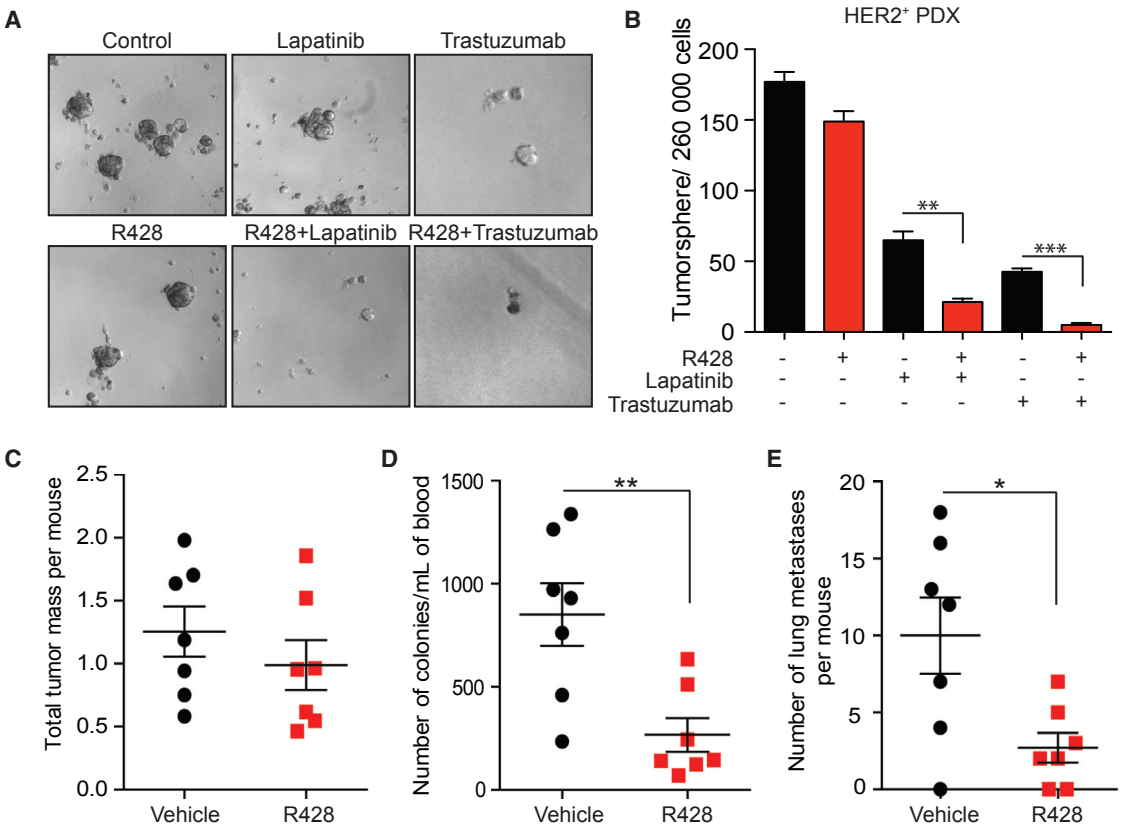

Figure 7. Prolonged Pharmacological Inhibition of AXL *In Vivo* in the MMTV-NIC HER2$^+$ Breast Cancer Model Reduces Metastasis

(A and B) Treatment of human HER2$^+$ PDX cells with a combination of R428 (0.5 μM) and lapatinib (0.5 μM) or trastuzumab (5 μg/mL) (A) abrogates tumorspheres formation (B). **p = 0.0063, ***p = 0.0002. Scale bar, 150 μm.

(C) *In vivo* R428 treatment does not have a significant effect on tumor mass in MMTV-NIC HER2$^+$ females. Data are represented as mean ± SEM.

(D and E) Treatment with the AXL inhibitor R428 reduces the number of circulating tumor cells (D) and lung metastases (E) in MMTV-NIC females. **p = 0.0054 and *p = 0.018.

See also Figure S7.

site *in vivo* (Patel and Rameshwar, 2013). We found that either lapatinib or trastuzumab reduced tumorsphere formation of our HER2$^+$ PDX cells, while R428 had a modest effect (Figures 7A and 7B). The combination of both AXL and HER2 inhibitors blunted the formation of tumorspheres (Figures 7A and 7B). In order to provide proof-of-principle that inhibition of AXL *in vivo* decreases metastatic burden, we used the MMTV-NIC mouse model of HER2$^+$ breast cancer. Cohorts of females were treated daily with either R428 or vehicle for 5 weeks after the appearance of the first palpable tumors. Prolonged exposure to R428 decreased AXL phosphorylation and also led to an upregulation of AXL (Figure S7H). At the end of the experiment, multiple tumor progression parameters were analyzed, and we determined that prolonged *in vivo* AXL inhibition mimicked its genetic deletion. Although we found no difference in the proliferation (Ki67), apoptosis (cleaved-caspase 3) or the total tumor mass

Figure 6. AXL Is Required for TGF-β-Induced Cell Invasion and Its Expression Is Linked to EMT and TGF-β Signaling in Human HER2$^+$ Tumors

(A) HCC1954 cells treated with TGF-β show an increase in AXL expression.

(B) Treatment with R428 or siAXL abrogates TGF-β induced cell invasion of HCC1954.

(C) AXL and HER2 forms a complex, as measured by PLA, in HCC1954-treated with TGF-β.

(D and E) Combination of R428 (1 μM) with lapatinib (1 μM) or trastuzumab (10 μg/mL) (D) reduces cell invasion of TGF-β-treated HCC1954 cells (E).

(F) AXL expression is induced by TGF-β treatment in HER2$^+$ PDX cells.

(G) AXL is required for TGF-β-induced cell invasion of HER2$^+$ PDX cells.

(H) PLA shows that AXL and HER2 interacts in PDX cells following TGF-β stimulation. Scale bar, 20 μm.

(I) Combination of R428 (1 μM) with lapatinib (1 μM) or trastuzumab (1 μg/mL) blocks cell invasion of TGF-β-treated HER2$^+$ PDX cells.

(J) High levels of AXL in human TMA correlate with EMT markers.

(K) Transcriptomics analyses of HER2$^+$ breast cancer patient samples reveal that AXL expression correlates with TGF-β signatures (n = 68).

See also Figures S6 and S7.

of R428-treated mice in comparison to mice that received vehicle alone (Figures 7C and S7I–S7L), R428 administration decreased the number of CTCs and the total lung metastatic burden of MMTV-NIC animals (Figures 7D and 7E). In summary, we report a preclinical model demonstrating that AXL is essential for the metastatic progression of HER2$^+$ breast cancer *in vivo*, and we suggest that AXL inhibition could be a powerful approach to limit metastatic spreading.

DISCUSSION

AXL expression is primarily limited to breast cancer cell lines representative of the triple-negative molecular subtypes, and virtually no expression is detectable in luminal or HER2$^+$ cell lines (D'Alfonso et al., 2014; Wilson et al., 2014). An emerging feature of AXL expression across multiple solid tumor cell lines is the link with EMT (i.e., cells expressing mesenchymal markers) (Antony et al., 2016; Wilson et al., 2014). These data have led to the establishment of AXL as a candidate marker of TNBC. In this study, we demonstrate that AXL is expressed in a subset of HER2$^+$ human breast cancers that display an EMT signature and this is linked to poor clinical outcome. Based on these data, we sought to determine if AXL plays a functional role and if it is an actionable target during HER2$^+$ breast cancer progression. Through a series of genetic and functional assays, we demonstrate a central role for AXL in promoting metastasis in the context of HER2$^+$ breast cancer.

An AXL decoy receptor with enhanced GAS6-binding properties, MYD1, was engineered as a therapeutic tool to disrupt GAS6/AXL signaling *in vivo* (Kariolis et al., 2014). MYD1 was shown to block metastasis of human ovarian cancer cells and a murine breast cancer cell line in grafting assays in mice. These data led to the notion that targeting GAS6 might be a novel approach to limit metastasis. In contrast, by using a genetic approach to characterize a pre-clinical breast cancer model, we found that GAS6, but not AXL, was dispensable for HER2-driven metastasis *in vivo*. These findings not only demonstrate that autocrine secretion of GAS6 from cancer cells is not required for metastasis, but also that GAS6 expressed in the lungs is not acting as a homing factor for the cancer cells in this model. Rather, AXL appears to physically interact with HER2, thereby bypassing the necessity for GAS6, and this leads to HER2-mediated transphosphorylation and activation of AXL that triggers cell invasion. Recent data suggest that AXL heterodimerization with other transmembrane receptors occurs in multiple pathophysiological contexts (Meyer et al., 2013; Ruan and Kazlauskas, 2012; Salian-Mehta et al., 2013). Our results provide mechanistic details demonstrating that the interaction of AXL with HER2 increases both AXL half-life and its localization at the cell surface. Interestingly, the formation of HER2/EGFR heterodimers has also been reported to stabilize EGFR at the cell surface leading to enhanced oncogenic signaling (Hendriks et al., 2003; Lenferink et al., 1998). Hence, ligand-independent activation of AXL could be a common event in cancers driven by RTKs. One implication of our findings is that determining the GAS6-dependency of tumors for metastasis may be important before considering therapeutic approaches that target the GAS6/AXL interaction. Unlike in humans, our murine models have the limitation that metastasis only occurs to lungs, therefore we cannot exclude the possibility that GAS6 could be important in controlling metastasis to other organs. In prostate cancer models, GAS6 expressed by the bone promotes a tumor cell dormancy state (Shiozawa et al., 2010). It will be important to determine if GAS6 is important for bone metastasis because it is a frequent site of dissemination in HER2$^+$ breast cancer patients. In addition, PROTEIN S (PROS1), a GAS6-related protein that preferentially activates TYRO3 and MERTK over AXL (Linger et al., 2008), is also expressed in murine HER2$^+$ tumors. Whether dual targeting of GAS6 and PROS1 would impact AXL-mediated metastasis remains to be tested.

The plasticity of EMT is critical to allow for efficient metastasis (Li and Kang, 2016; Aceto et al., 2015). Acquisition of EMT features facilitates migration within the primary tumor and intravasation (Giampieri et al., 2009), prepares the cells in the circulation for extravasation (Labelle et al., 2011), and is required for extravasation (Padua and Massagué, 2009). AXL is frequently expressed in cancer cells of various origins that display mesenchymal features (Gjerdrum et al., 2010; Wu et al., 2014). While there is now substantial evidence to suggest that AXL is a promoter of metastasis in solid cancers, its contributions to the various steps of the metastatic process as an effector of EMT and throughout the metastatic cascade have not been dissected. While HER2$^+$ cancers retain epithelial features, the progression to the metastatic stage is thought to require EMT (Wu et al., 2016). We report here that AXL is essential for the intravasation of HER2$^+$ cancer cells, as measured by quantifying the CTCs in both immune-competent and immune-compromised mice. We confirmed the contribution of AXL to EMT-induced invasion in multiple models, in particular using a human the HER2$^+$ cell line HCC1954 and the HER2$^+$ PDX cell. Interestingly, the HER2$^+$ PDX cells used in this study does not express AXL and mesenchymal markers in basal conditions like other HER2$^+$ breast cancer cell lines studied to date (D'Alfonso et al., 2014; Wilson et al., 2014), unless they are reprogrammed by TGF-β. We also found that AXL is a mediator of TGF-β-induced extravasation of HER2$^+$ cancer cells. Hence, AXL may be needed to allow for efficient TGF-β-reprogramming of cells for extravasation. Our findings that AXL is essential for extravasation in HER2$^+$ cancer cells are in agreement with several experimental metastasis assays that have suggested a role for AXL in the extravasation of triple-negative breast cancer cells (Vuoriluoto et al., 2011). However, the major difference is that triple-negative breast cancer cells are initially mesenchymal and express high AXL while HER2$^+$ cells must undergo EMT for AXL expression and AXL-mediated extravasation.

By performing knockdown of AXL once HER2$^+$ cancer cells have achieved lung colonization, we demonstrated that AXL contributes to the establishment of macrometastases. While inhibition of AXL impairs the efficiency of metastasis, the later finding has major clinical implications since pharmacological inhibition of AXL even at later stages may have the potential to reduce metastatic outgrowth. A recent study using tumor initiating cells from PyMT transgenic mouse tumors that display partial EMT (AXL$^+$) suggested that AXL, by promoting the secretion of THBS2 and activation of fibroblasts, prepares the metastatic niche (Del Pozo Martin et al., 2015). We found that *THBS2* was downregulated in the Axl$^{-/-}$ tumors (Figure 5D), in agreement

with a role for AXL in the niche activation. These data support the notion that inhibition of AXL in HER2$^+$ breast cancer dampens the efficiency of every step of the metastatic cascade.

Most patients afflicted with HER2$^+$ breast cancer undergo first line therapy with agents that target HER2. We tested the effect of prolonged systemic pharmacological inhibition of AXL and found that R428 treatments phenocopied the genetic deletion of AXL, i.e., a decrease in both CTCs and lung metastases with no effect on primary tumor growth. Furthermore, co-treatment with R428 and HER2 blocking agents inhibited HER2$^+$ PDX tumorspheres growth. Collectively, our data demonstrate that anti-AXL therapy is sufficient to reduce metastasis in HER2$^+$ cancers in experimental models. It will be key to define pre-clinical conditions to determine if co-targeting of HER2 and AXL affects tumor growth, intravasation and extravasation, and survival of the DTCs.

EXPERIMENTAL PROCEDURES

Tumor Microarrays

A cohort of 300 female breast cancer patients comprising ductal and medullary tumors specimen of different histological grades was used in the retrospective study. Formalin-fixed, paraffin-embedded (FFPE) samples containing tumor tissues were collected for the study and prepared as tumor microarrays (TMA) at IRIC Histology core facility. Tumor grades were confirmed using the Modified Scarff-Bloom-Richardson-Elston-Ellis grading system. Information on the TMA and the follow-up data, including the onset of metastasis and relapse are described in Yousef et al. (2014). The Human Ethics Committee of the Université de Montréal Hospital Center (3SL05.019) approved the use of these specimens and research data.

Animal Experiments

Mice were housed in a specific pathogen-free (SPF) facility and experiments were approved by the Animal Care Committee of the Institut de Recherches Cliniques de Montréal and complied with the Canadian Council of Animal Care guidelines.

Statistics

Data are presented as mean ± SEM from at least 3 independent experiments. Statistical analyses were performed with the GraphPad Prism Software using the Student's t test (comparison of two independent groups) or Chi-square. p values <0.05 were considered as significant (*$p < 0.05$, **$p < 0.001$, ***$p < 0.0001$).

DATA AND SOFTWARE AVAILABILITY

The accession numbers for the RNA-seq reported in this paper are GEO: GSE102370 (mouse tumors) and GSE58644 (human breast cancer cohort). Mendeley https://doi.org/10.17632/xjwbwrb35k.1.

SUPPLEMENTAL INFORMATION

Supplemental Information includes Supplemental Experimental Procedures, seven figures, two tables, and two videos and can be found with this article online at https://doi.org/10.1016/j.celrep.2018.04.019.

ACKNOWLEDGMENTS

We thank Drs. Frédéric Charron, Mathieu Ferron, and Mélanie Laurin for critical reading of the manuscript. We thank Drs. Tatiana Smirnova and Jeffrey E. Segall (Albert Einstein College, USA) for their generous advice to measure circulating tumor cells. We thank Manon Laprise, Marie-Claude Lavallée, and Suzie Riverin for their technical assistance with mice, Dominic Filion for microscopy assistance, and Simone Terouz for histology. This work was supported by operating grants from the Canadian Institute of Health Research (MOP-142425 to J.F.C. and J.P.G and MOP-142374 to P.P.R.), the Réseau de Recherche en Cancer of the FRQS (FRQ-34787), and Quebec Breast Cancer Foundation (to M.P.). M.-A.G. is a recipient of a CIHR Doctoral studentship. L.A. is a recipient of a Cole Foundation Postdoctoral Fellowship. M.P. holds the Diane and Sal Guerrera Chair in Cancer Genomics at McGill University. J.F.C. holds the Transat Chair in Breast Cancer Research. P.P.R. and J.-F.C. are supported by FRQS Senior investigator career awards.

AUTHOR CONTRIBUTIONS

Conceptualization, M.-A.G., J.-P.G., and J.-F.C.; Methodology, M.-A.G., L.A., A.P., P.S., R.M.J., P.P.R., and J.-F.C.; Investigation, M.-A.G., S.D., M.-P.T., L.A., A.P., P.S., and R.M.J.; Formal Analysis, M.-A.G., L.A., and R.M.J.; Resources, W.J.M., P.C., M.B., and L.G.; Writing – Original Draft, M.-A.G. and J.-F.C.; Writing – Review & Editing, M.-A.G., W.J.M., P.C., P.P.R., M.P., J.-P.G., and J.-F.C.; Supervision, M.P, P.P.R., and J.-F.C.; Funding Acquisition, J.-P.G. and J.-F.C.

DECLARATION OF INTERESTS

The authors declare no competing interests.

Received: August 31, 2017
Revised: February 21, 2018
Accepted: April 3, 2018
Published: May 1, 2018

REFERENCES

Antony, J., Tan, T.Z., Kelly, Z., Low, J., Choolani, M., Recchi, C., Gabra, H., Thiery, J.P., and Huang, R.Y. (2016). The GAS6-AXL signaling network is a mesenchymal (Mes) molecular subtype-specific therapeutic target for ovarian cancer. Sci. Signal. *9*, ra97.

Asiedu, M.K., Beauchamp-Perez, F.D., Ingle, J.N., Behrens, M.D., Radisky, D.C., and Knutson, K.L. (2014). AXL induces epithelial-to-mesenchymal transition and regulates the function of breast cancer stem cells. Oncogene *33*, 1316–1324.

Bose, R., Molina, H., Patterson, A.S., Bitok, J.K., Periaswamy, B., Bader, J.S., Pandey, A., and Cole, P.A. (2006). Phosphoproteomic analysis of Her2/neu signaling and inhibition. Proc. Natl. Acad. Sci. USA *103*, 9773–9778.

Brenton, J.D., Carey, L.A., Ahmed, A.A., and Caldas, C. (2005). Molecular classification and molecular forecasting of breast cancer: ready for clinical application? J. Clin. Oncol. *23*, 7350–7360.

D'Alfonso, T.M., Hannah, J., Chen, Z., Liu, Y., Zhou, P., and Shin, S.J. (2014). Axl receptor tyrosine kinase expression in breast cancer. J. Clin. Pathol. *67*, 690–696.

De Laurentiis, M., Cancello, G., Zinno, L., Montagna, E., Malorni, L., Esposito, A., Pennacchio, R., Silvestro, L., Giuliano, M., Giordano, A., et al. (2005). Targeting HER2 as a therapeutic strategy for breast cancer: a paradigmatic shift of drug development in oncology. Ann. Oncol. *16* (*Suppl 4*), iv7–13.

Del Pozo Martin, Y., Park, D., Ramachandran, A., Ombrato, L., Calvo, F., Chakravarty, P., Spencer-Dene, B., Derzsi, S., Hill, C.S., Sahai, E., and Malanchi, I. (2015). Mesenchymal cancer cell-stroma crosstalk promotes niche activation, epithelial reversion, and metastatic colonization. Cell Rep. *13*, 2456–2469.

Giampieri, S., Manning, C., Hooper, S., Jones, L., Hill, C.S., and Sahai, E. (2009). Localized and reversible TGFbeta signalling switches breast cancer cells from cohesive to single cell motility. Nat. Cell Biol. *11*, 1287–1296.

Gjerdrum, C., Tiron, C., Høiby, T., Stefansson, I., Haugen, H., Sandal, T., Collett, K., Li, S., McCormack, E., Gjertsen, B.T., et al. (2010). Axl is an essential epithelial-to-mesenchymal transition-induced regulator of breast cancer metastasis and patient survival. Proc. Natl. Acad. Sci. USA *107*, 1124–1129.

Graham, D.K., DeRyckere, D., Davies, K.D., and Earp, H.S. (2014). The TAM family: phosphatidylserine sensing receptor tyrosine kinases gone awry in cancer. Nat. Rev. Cancer *14*, 769–785.

Hendriks, B.S., Opresko, L.K., Wiley, H.S., and Lauffenburger, D. (2003). Coregulation of epidermal growth factor receptor/human epidermal growth factor

receptor 2 (HER2) levels and locations: quantitative analysis of HER2 overexpression effects. Cancer Res. *63*, 1130–1137.

Jin, G., Wang, Z., Wang, J., Zhang, L., Chen, Y., Yuan, P., and Liu, D. (2017). Expression of Axl and its prognostic significance in human breast cancer. Oncol. Lett. *13*, 621–628.

Kariolis, M.S., Miao, Y.R., Jones, D.S., 2nd, Kapur, S., Mathews, I.I., Giaccia, A.J., and Cochran, J.R. (2014). An engineered Axl 'decoy receptor' effectively silences the Gas6-Axl signaling axis. Nat. Chem. Biol. *10*, 977–983.

Kedrin, D., van Rheenen, J., Hernandez, L., Condeelis, J., and Segall, J.E. (2007). Cell motility and cytoskeletal regulation in invasion and metastasis. J. Mammary Gland Biol. Neoplasia *12*, 143–152.

Kwong, K.Y., and Hung, M.C. (1998). A novel splice variant of HER2 with increased transformation activity. Mol. Carcinog. *23*, 62–68.

Labelle, M., Begum, S., and Hynes, R.O. (2011). Direct signaling between platelets and cancer cells induces an epithelial-mesenchymal-like transition and promotes metastasis. Cancer Cell *20*, 576–590.

Lambert, A.W., Pattabiraman, D.R., and Weinberg, R.A. (2017). Emerging biological principles of metastasis. Cell *168*, 670–691.

Laurin, M., Huber, J., Pelletier, A., Houalla, T., Park, M., Fukui, Y., Haibe-Kains, B., Muller, W.J., and Côté, J.F. (2013). Rac-specific guanine nucleotide exchange factor DOCK1 is a critical regulator of HER2-mediated breast cancer metastasis. Proc. Natl. Acad. Sci. USA *110*, 7434–7439.

Leconet, W., Chentouf, M., Du Manoir, S., Chevalier, C., Sirevnt, A., Ait-Arsa, I., Busson, M., Jarlier, M., Radosevic-Robin, N., Theillet, C.G., et al. (2016). Therapeutic activity of anti-AXL antibody against triple-negative breast cancer patient derived xenografts and metastasis. Clin. Cancer Res. *23*, 2806–2816.

Lemke, G., and Rothlin, C.V. (2008). Immunobiology of the TAM receptors. Nat. Rev. Immunol. *8*, 327–336.

Lenferink, A.E., Pinkas-Kramarski, R., van de Poll, M.L., van Vugt, M.J., Klapper, L.N., Tzahar, E., Waterman, H., Sela, M., van Zoelen, E.J., and Yarden, Y. (1998). Differential endocytic routing of homo- and hetero-dimeric ErbB tyrosine kinases confers signaling superiority to receptor heterodimers. EMBO J. *17*, 3385–3397.

Li, W., and Kang, Y. (2016). Probing the fifty shades of EMT in metastasis. Trends Cancer *2*, 65–67.

Linger, R.M., Keating, A.K., Earp, H.S., and Graham, D.K. (2008). TAM receptor tyrosine kinases: biologic functions, signaling, and potential therapeutic targeting in human cancer. Adv. Cancer Res. *100*, 35–83.

Lozneanu, L., Pinciroli, P., Ciobanu, D.A., Carcangiu, M.L., Canevari, S., Tomassetti, A., and Căruntu, I.D. (2016). Computational and immunohistochemical analyses highlight AXL as a potential prognostic marker for ovarian cancer patients. Anticancer Res. *36*, 4155–4163.

Mc Cormack, O., Chung, W.Y., Fitzpatrick, P., Cooke, F., Flynn, B., Harrison, M., Fox, E., Gallagher, E., Goldrick, A.M., Dervan, P.A., et al. (2008). Growth arrest-specific gene 6 expression in human breast cancer. Br. J. Cancer *98*, 1141–1146.

Meyer, A.S., Miller, M.A., Gertler, F.B., and Lauffenburger, D.A. (2013). The receptor AXL diversifies EGFR signaling and limits the response to EGFR-targeted inhibitors in triple-negative breast cancer cells. Sci. Signal. *6*, ra66.

Mukohara, T. (2011). Mechanisms of resistance to anti-human epidermal growth factor receptor 2 agents in breast cancer. Cancer Sci. *102*, 1–8.

Aceto, N., Toner, M., Maheswaran, S., and Haber, D.A. (2015). En route to metastasis: circulating tumor cell clusters and epithelial-to-mesenchymal transition. Trends Cancer *1*, 45–52.

O'Bryan, J.P., Frye, R.A., Cogswell, P.C., Neubauer, A., Kitch, B., Prokop, C., Espinosa, R., 3rd, Le Beau, M.M., Earp, H.S., and Liu, E.T. (1991). axl, a transforming gene isolated from primary human myeloid leukemia cells, encodes a novel receptor tyrosine kinase. Mol. Cell. Biol. *11*, 5016–5031.

Padua, D., and Massagué, J. (2009). Roles of TGFbeta in metastasis. Cell Res. *19*, 89–102.

Patel, S., and Rameshwar, P. (2013). Tumorsphere passage for breast cancer stem cells. Protoc. Exchange. https://doi.org/10.1038/protex.2013.023.

Rankin, E.B., Fuh, K.C., Taylor, T.E., Krieg, A.J., Musser, M., Yuan, J., Wei, K., Kuo, C.J., Longacre, T.A., and Giaccia, A.J. (2010). AXL is an essential factor and therapeutic target for metastatic ovarian cancer. Cancer Res. *70*, 7570–7579.

Rothlin, C.V., Ghosh, S., Zuniga, E.I., Oldstone, M.B., and Lemke, G. (2007). TAM receptors are pleiotropic inhibitors of the innate immune response. Cell *131*, 1124–1136.

Ruan, G.X., and Kazlauskas, A. (2012). Axl is essential for VEGF-A-dependent activation of PI3K/Akt. EMBO J. *31*, 1692–1703.

Salian-Mehta, S., Xu, M., and Wierman, M.E. (2013). AXL and MET crosstalk to promote gonadotropin releasing hormone (GnRH) neuronal cell migration and survival. Mol. Cell. Endocrinol. *374*, 92–100.

Seal, M.D., and Chia, S.K. (2010). What is the difference between triple-negative and basal breast cancers? Cancer J. *16*, 12–16.

Shieh, Y.S., Lai, C.Y., Kao, Y.R., Shiah, S.G., Chu, Y.W., Lee, H.S., and Wu, C.W. (2005). Expression of axl in lung adenocarcinoma and correlation with tumor progression. Neoplasia *7*, 1058–1064.

Shiozawa, Y., Pedersen, E.A., Patel, L.R., Ziegler, A.M., Havens, A.M., Jung, Y., Wang, J., Zalucha, S., Loberg, R.D., Pienta, K.J., and Taichman, R.S. (2010). GAS6/AXL axis regulates prostate cancer invasion, proliferation, and survival in the bone marrow niche. Neoplasia *12*, 116–127.

Siegel, P.M., Ryan, E.D., Cardiff, R.D., and Muller, W.J. (1999). Elevated expression of activated forms of Neu/ErbB-2 and ErbB-3 are involved in the induction of mammary tumors in transgenic mice: implications for human breast cancer. EMBO J. *18*, 2149–2164.

Siegel, P.M., Shu, W., Cardiff, R.D., Muller, W.J., and Massagué, J. (2003). Transforming growth factor beta signaling impairs Neu-induced mammary tumorigenesis while promoting pulmonary metastasis. Proc. Natl. Acad. Sci. USA *100*, 8430–8435.

Tsai, J.H., and Yang, J. (2013). Epithelial-mesenchymal plasticity in carcinoma metastasis. Genes Dev. *27*, 2192–2206.

Ursini-Siegel, J., Hardy, W.R., Zuo, D., Lam, S.H., Sanguin-Gendreau, V., Cardiff, R.D., Pawson, T., and Muller, W.J. (2008). ShcA signalling is essential for tumour progression in mouse models of human breast cancer. EMBO J. *27*, 910–920.

Visvader, J.E. (2009). Keeping abreast of the mammary epithelial hierarchy and breast tumorigenesis. Genes Dev. *23*, 2563–2577.

Vuoriluoto, K., Haugen, H., Kiviluoto, S., Mpindi, J.P., Nevo, J., Gjerdrum, C., Tiron, C., Lorens, J.B., and Ivaska, J. (2011). Vimentin regulates EMT induction by Slug and oncogenic H-Ras and migration by governing Axl expression in breast cancer. Oncogene *30*, 1436–1448.

Wilson, C., Ye, X., Pham, T., Lin, E., Chan, S., McNamara, E., Neve, R.M., Belmont, L., Koeppen, H., Yauch, R.L., et al. (2014). AXL inhibition sensitizes mesenchymal cancer cells to antimitotic drugs. Cancer Res. *74*, 5878–5890.

Wu, F., Li, J., Jang, C., Wang, J., and Xiong, J. (2014). The role of Axl in drug resistance and epithelial-to-mesenchymal transition of non-small cell lung carcinoma. Int. J. Clin. Exp. Pathol. *7*, 6653–6661.

Wu, X., Zahari, M.S., Ma, B., Liu, R., Renuse, S., Sahasrabuddhe, N.A., Chen, L., Chaerkady, R., Kim, M.S., Zhong, J., et al. (2015). Global phosphotyrosine survey in triple-negative breast cancer reveals activation of multiple tyrosine kinase signaling pathways. Oncotarget *6*, 29143–29160.

Wu, Y., Sarkissyan, M., and Vadgama, J.V. (2016). Epithelial-mesenchymal transition and breast cancer. J. Clin. Med. *5*, E13.

Wu, X., Ma, W., Zhou, Q., Yan, H., Lim, Z.F., Huang, M., Deng, C., Yu, X., Su, H., Komo, S., et al. (2017). AXL-GAS6 expression can predict for adverse prognosis in non-small cell lung cancer with brain metastases. J. Cancer Res. Clin. Oncol. *143*, 1947–1957.

Yousef, E.M., Tahir, M.R., St-Pierre, Y., and Gaboury, L.A. (2014). MMP-9 expression varies according to molecular subtypes of breast cancer. BMC Cancer *14*, 609.

Yu, H., Liu, R., Ma, B., Li, X., Yen, H.Y., Zhou, Y., Krasnoperov, V., Xia, Z., Zhang, X., Bove, A.M., et al. (2015). Axl receptor tyrosine kinase is a potential therapeutic target in renal cell carcinoma. Br. J. Cancer *113*, 616–625.